

PS Surge Propagation in Debris Flows*

Paul Allen¹, Oliver Harlen², Robert Dorrell³, Robert Thomas⁴, and William McCaffrey⁴

Search and Discovery Article #51540 (2018)**

Posted November 12, 2018

*Adapted from poster presentation given at AAPG 2018 Annual Convention & Exhibition, Salt Lake City, Utah, United States, May 20-23, 2018

**Datapages © 2018. Serial rights given by author. For all other rights contact author directly. DOI:10.1306/51540Allen2018

¹School of Computing, University of Leeds, Leeds, West Yorkshire, United Kingdom (scpaa@leeds.ac.uk)

²School of Mathematics, University of Leeds, Leeds, United Kingdom

³University of Hull, Hull, United Kingdom

⁴School of Earth and Environment, University of Leeds, Leeds, United Kingdom

Abstract

Submarine debris flows and associated turbidity currents are important geohazards that may damage seafloor infrastructure, whilst their deposits form important heterogeneities in many deep marine turbidite reservoirs. Turbidity current models are sensitive to the required prescribed initial conditions and although the mechanics of both laminar (non-Newtonian) debris flows and turbulent (Newtonian) turbidity currents have been extensively studied, the transition from laminar to turbulent states is poorly described by current theory. Thus understanding the transition from high to low concentration is essential for turbidity currents initiated by an underwater landslide. This work presents a coupled experimental and numerical study of designed to provide new insight into this transition and sediment transport.

The experiments entailed the release of dyed glycerol and water mixtures of varying concentrations into a 5 m long, 0.25 m wide tank via the phased removal of two pneumatically-controlled lock gates. The phased release generated a laminar flow with an internal surge. The surge propagated as a bore on the upper flow surface that, for certain concentrations, caused an abrupt transition from a relatively dense laminar flow to a dense turbulent flow upon reaching the flow front. For higher concentrations, the pulse did not transfer sufficient energy to transition the flow; for lower concentrations, the flow front transitioned through mixing and erosion before the pulse reached the front.

Numerical simulations were undertaken with single-layer and two-layer Lagrangian finite-difference schemes based on the depth-averaged, shallow water equations. Layers were coupled through additional hydrostatic pressure and inter-layer drag terms. Both formulations qualitatively captured some key flow features, but the two-layer formulation more accurately replicated experimental observations. The present work exposes the limitations of depth-averaged numerical models, but also demonstrates the promise in constraining the role of intra-flow surges in debris flow transition.

Felix and Peakall (2006) proposed that six transformation mechanisms could operate, singly or in combination, during the evolution of debris flows into

turbidity currents. Three of these - erosion, mixing at the head and wave instability, are observed in the experiments. We assess the relative transformation efficiency of these mechanisms, and discuss the implications for the rock record.

References Cited

Bonnecaze, R.T., H.E. Huppert, and J.R. Lister, 1993, Particle-driven gravity currents: *Journal of Fluid Mechanics*, v. 250, p.339-369.

Cheng, N.S., 2008, Formula for the viscosity of a glycerol– water mixture: *Industrial & Engineering Chemistry Research*, v. 47/9, p.3285-3288.

Felix, M. and J. Peakall, 2006, Transformation of debris flows into turbidity currents: mechanisms inferred from laboratory experiments: *Sedimentology*, v. 53/1, p.107-123.

Surge propagation in debris flows

Paul Allen¹, Oliver Harlen, Robert Dorrell, Robert Thomas, William McCaffrey

¹- School of Computing, University of Leeds, Leeds LS2 9JT, UK. Email: scpaa@leeds.ac.uk

ConocoPhillips

HESS

MURPHY

Shell

enl

AkerBP

Statoil

Submarine debris flows are high density gravity flows caused by underwater landslides. They are a potential geohazard to telecommunication cables, pipelines and seafloor equipment, such as well heads. They may also transform into turbidity currents (more dilute flows characterised by the preferential settling of larger grains), whose deposits can hold hydrocarbon reservoirs [1]. Current theory does not capture well the transition between laminar (non-Newtonian) and turbulent (Newtonian) rheological states; further insight is required to enable more accurate hazard prediction and to maximise economic benefit. Surges are inherent to debris flows and may play a role in flow transformation. This work investigates the effect of flow surges on laminar to turbulent transformation in the phased release of dilute glycerol gravity currents, through a double lockgate release.

1. Introduction

- Gravity currents are flows driven by a density difference, for example turbidity currents and debris flows. Suspended sediment causes the excess density for these flows.
- Fluid turbulence suspends the particles in turbidity currents and graded deposits (turbidites, Figure 1) are produced, which can form hydrocarbon reservoirs, by the preferential settling of larger grains.
- Particles in a debris flow are supported by a matrix strength. The particle size distribution is broader with particles ranging from microns to metres.
- Debris flows are generally well mixed and unstratified and the deposits (debrites Figure 1) are associated with en masse settling.
- Debris flows and turbidity currents are a geohazard and can cause damage to telecommunication cables, pipelines and seafloor equipment, such as well heads. Further, debris flows can erode potential reservoirs and create internal barriers and baffles creating heterogeneities comprising



Figure 1: Turbidite (top) consists of fining upwards sandy deposits T_a , T_b and T_c followed by a layer of siltstone T_d and finally mudstone T_e . The Debrite (bottom) is unstratified and poorly sorted with a much wider range of particle sizes.

Turbidity currents are Newtonian meaning that a linear relationship between stress and shear-rate exists. In contrast debris flows exhibit both a non-linear relationship between stress and shear-rate and the existence of a non-zero yield strength, i.e. a non-zero amount of stress is required before there is any shear. The non-Newtonian behaviour of the debris flow creates a more 'plug-like' flow, Figure 2.

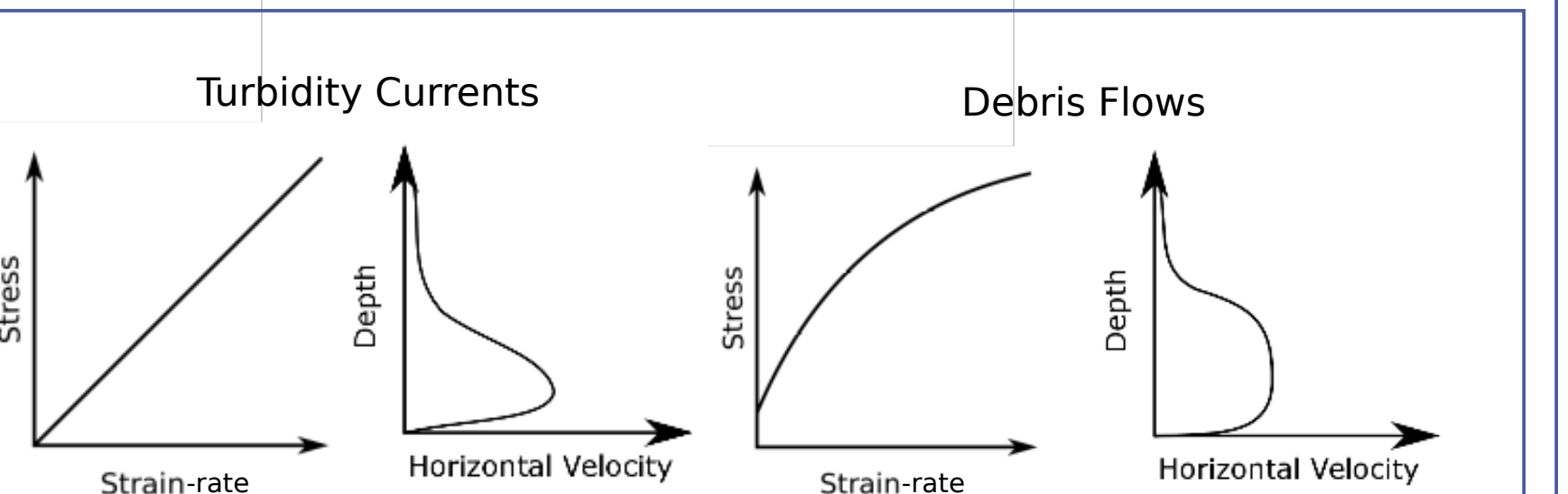
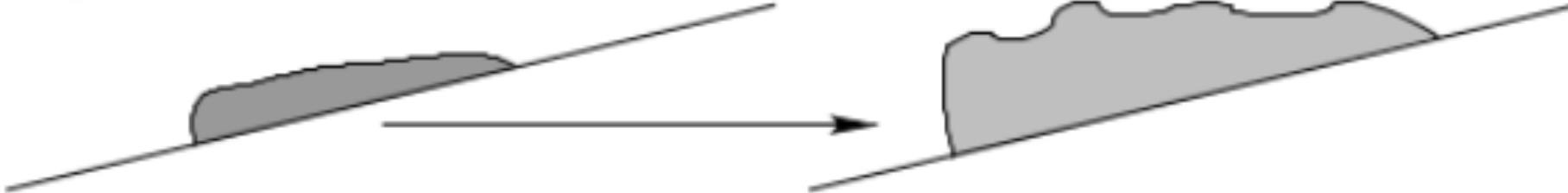


Figure 2: Example stress-strain-rate relationships and horizontal velocity profiles for turbidity currents (left) and debris flows (right). The yield strength and shear-thinning (decreasing gradient) will create a more 'plug-like' velocity profile in the debris flow.

In reality turbidity currents and debris flows represent end members of a spectrum of flows. Debris flows may transition into turbidity currents and as result of geohazards represented by these flows and their economic significance to connected industry, understanding the transformation process and conditions for is critical.

A Liquefaction



A: Absorption of water into part or all of the flow is known as liquefaction. The current slowly becomes more dilute and turbulent as more water is absorbed.

B Breaking up of flow



B: Progressive disintegration of the flow into smaller and smaller pieces.

C Shear on top leads to erosion



C: Shear on top by the ambient water leading to erosion.

D Mixing due to instability and wave formation at the surface



D: Kelvin-Helmholtz-like instability that appears as surface waves that may break, which enhances shear and mixing.

E Hydraulic jump



E: Rapid and localised transition usually caused by a change in bed topography and the rapid deposition of sediment.

F Mixing under and into the head of the flow



F: Water forced underneath the head mixes and is absorbed underneath the current.

Felix and Peakall (2006) [1] discussed six proposed mechanisms detailed above. Liquefaction and dilution through a hydraulic jump are not efficient transformation mechanisms over short time scales, whereas the other four (circled) may or may not be depending on flow composition or bed topography. An efficient transformation suspends the majority of the sediment in the debris flow into the turbidity current. Further, the efficient mechanisms may transform over significantly long periods of time in contrast to the both rapid and efficient transformations that are inferred from deposits.

Surges are an inherent feature of both sub-aerial and sub-aqueous debris flows. Surges can arise allogically, through the combining of multiple flows or failures, or autogenically through instabilities and the variable supply of dense material. Surges can transfer energy to the head of the flow significantly affecting the transformation mechanisms, and their time scales. The disturbance by the surge wave, in general, travel faster than the head and these internal velocity peaks affect erosional and depositional patterns within the current. Thus we seek to explore surge propagation in debris flows through idealised experiments and numerical models.

References

- [1] Felix, M. and Peakall, J., 2006. Transformation of debris flows into turbidity currents: mechanisms inferred from laboratory experiments. *Sedimentology*, 53(1), pp.107-123.
- [2] Cheng, N.S., 2008. Formula for the viscosity of a glycerol-water mixture. *Industrial & engineering chemistry research*, 47(9), pp.3285-3288.
- [3] Bonnecaze, R.T., Huppert, H.E. and Lister, J.R., 1993. Particle-driven gravity currents. *Journal of Fluid Mechanics*, 250, pp.339-369.

2. Laboratory Simulations

- Quasi-laminar gravity currents were created using a lock-exchange configuration, Figure 4. The proposed transformations mechanisms of Felix and Peakall (2006) and their efficiency were assessed.
- Glycerol-water mixtures at high concentrations were used to create the density difference.
- The high viscosity of glycerol-water mixtures created an initially laminar gravity current that minimised the turbulent mixing and entrainment. However a relatively diluted turbulent cloud is still observed, Figure 5.
- The head of the current slowly dilutes and becomes fully turbulent, Figure 5.
- Phased release of two lock-boxes created a gravity current with an internal surge. The gate separation time t_{re} was adjusted to created different sizes of surge, enabling us to explore the effect of surges on the transformation mechanisms.
- For a preliminary experiment at 80% glycerol concentration the surge transferred enough energy to the head to cause a rapid laminar to turbulent transition.

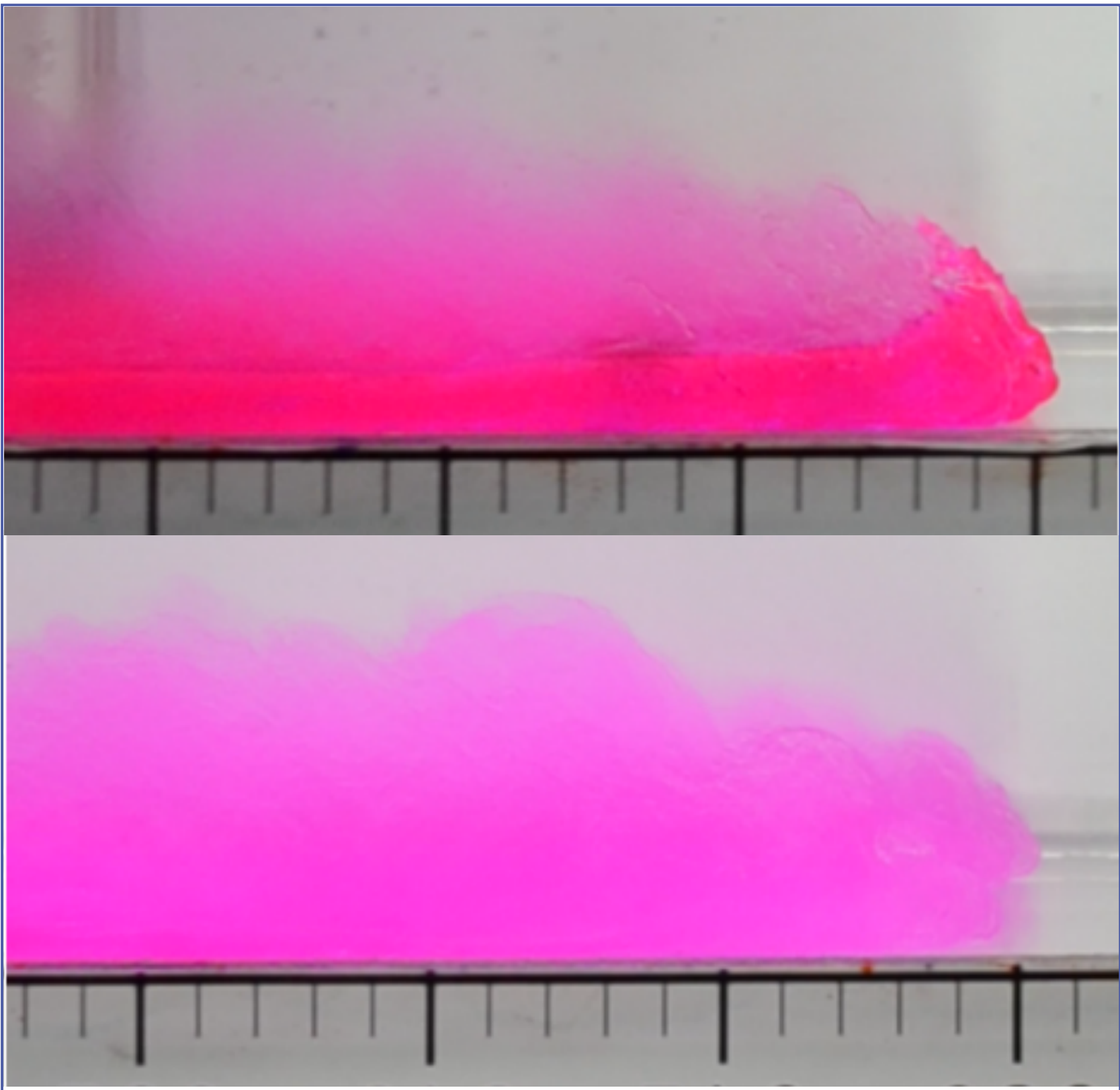


Figure 5: Laminar head with a dilute turbulent cloud created by mixing (top). Fully turbulent and dilute head (bottom). Scale in cm.

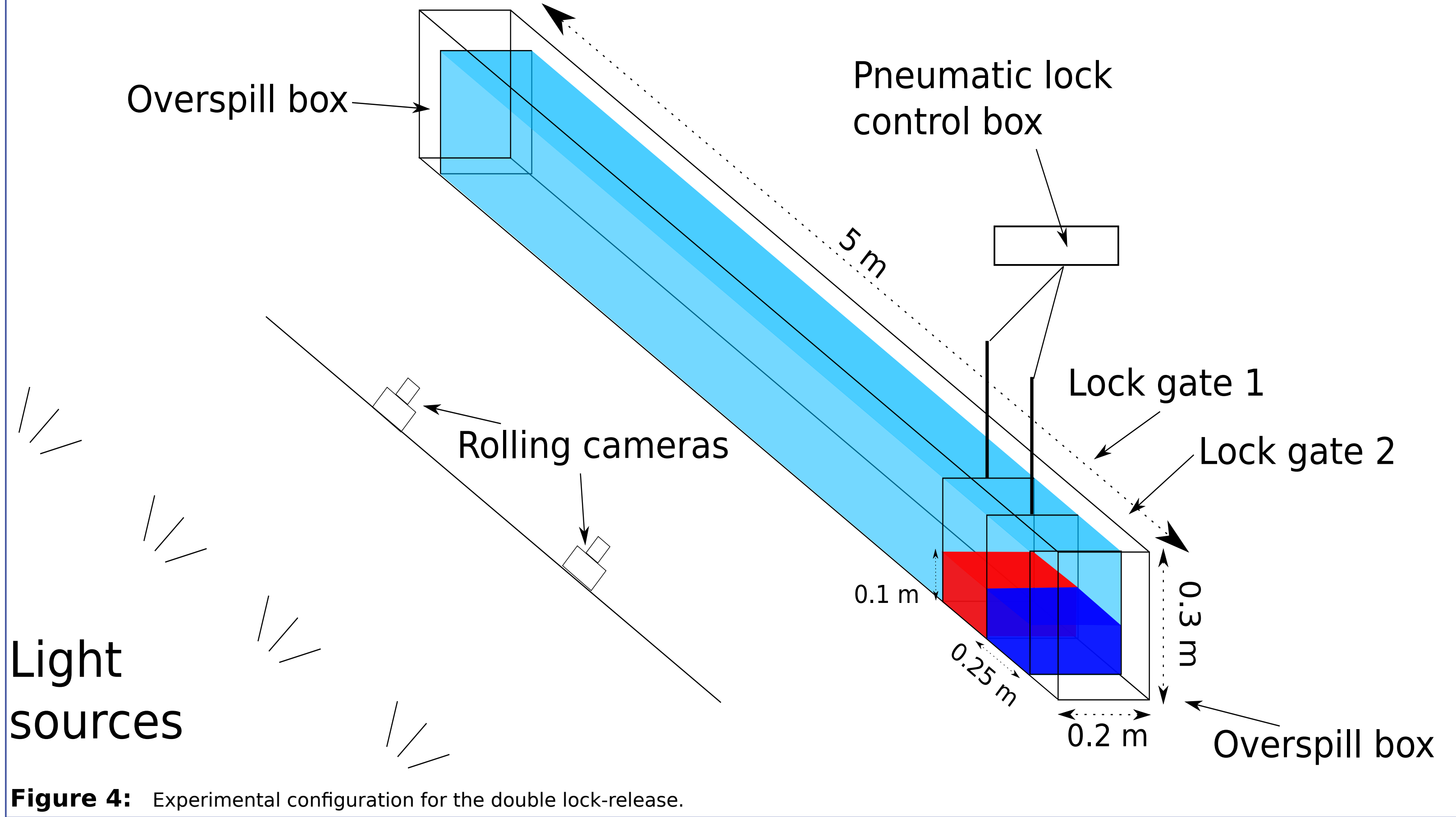


Figure 4: Experimental configuration for the double lock-release.

| | | Concentration | | |
|--------------------|-----|---------------|------|------|
| | | 77% | 84% | 90% |
| Fraction remaining | 1/2 | 1.5 | 1.35 | 1.3* |
| | 3/8 | - | 1.85 | 1.9* |
| | 1/4 | - | 2.85 | 3.3* |
| | 1/8 | - | 5 | 13.3 |

Table 1: Release times (s) for the experimental cases conducted with the sliding cameras. The asterisks indicate the experiments that were additionally conducted with the high-speed camera. 3/8, 1/4 and 1/8 were not conducted at the lowest concentration, 77%, because the flow mixed with the ambient too rapidly.

Experimental Methodology

A horizontal perspex tank of length 5 m, width 0.2 m and depth 0.3 m, Figure 4, with two lock-boxes of length 0.25 m at one end was filled with tap water to a depth of 0.25 m. A peristaltic pump was used to slowly fill the lock boxes to a depth $h_{lock}=0.1$ m, minimising the mixing with the ambient. The displaced fluid was caught in overspill boxes created by placing a 0.25 m deep perspex sheets 0.1 m from each end. The overspill boxes enabled surface waves to dissipate over the top rather than reflect off the ends of the tank.

A pneumatic lock control box controlled the withdrawal of the lock gates to ensure consistency. The speed was adjusted during a series of test runs to remove the gates quickly, whilst minimising the disturbance created by withdrawal. When two lock-gates were present the time between gate releases t_{re} was specified. The delayed release created a surge which travelled through to the front of the current.

Glycerol water mixtures are highly temperature dependent [2] and therefore, tap water was stored in storage tanks for at least 48 hours before being used in the experiments. The lab was temperature controlled and this ensured that the ambient water attained a relatively constant temperature throughout the experiments. Further, the glycerol mixtures were pre-mixed in a 200 litre mixing tank and left overnight to normalise to room temperature. Mixing entrained a limited amount of air into the mixture, which dissipated overnight.

Three different concentrations of glycerol were chosen to give a range of different Reynolds numbers, $Re_t = \sqrt{g'h_{lock}^3}/2\nu$ where g' is the buoyancy adjusted gravity and ν is the kinematic viscosity. The Reynolds number is the ratio between inertial and viscous forces and is a critical parameter in determining whether a flow will be turbulent or laminar. Using the parameterisation of Cheng (2008) [2], and assuming room temperature of 20°C, the required glycerol concentration was computed for three target Reynolds numbers within the laminar-transitional regime, $Re_t = 100, 200$ & 400. Gate separation times were based on the fractions (1/2, 3/8, 1/4 and 1/8) of fluid remaining in the first lock when the second gate was released, and displayed in Table 1.

The evolving flows were filmed with a pair of sliding cameras that tracked the head and the surge throughout the entire flow duration. Three release times at the highest concentration were performed again with a fixed high-speed camera that captured the flow in HD at 200 Hz and focused on the surge transition region, 12-70 cm downstream.

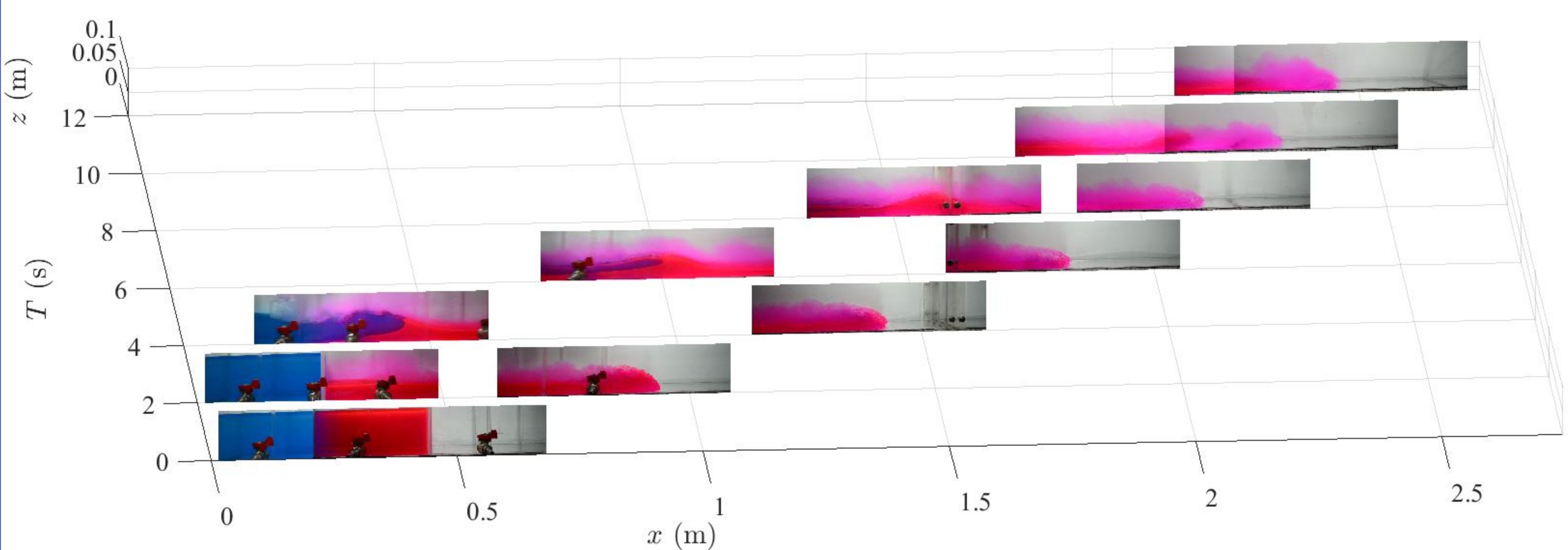


Figure 7: Development of the surge and head as filmed by the two sliding cameras displayed in intervals of 2 s with glycerol concentration 0.84 and gate separation time 2.85 s. The head was observed to be fully dilute by $t=8$ s before the surge arrived between 10 and 12 s.

- Filming with two sliding cameras enabled us to capture critical parts of the flow throughout the event. Stills from the pair of cameras for a single experiment of concentration 84% and $t_{re}=2.85$ s are displayed in Figure 7.
- A surge was created that propagated towards the front of the flow, but the head has already transitioned to turbulent before reaching it.
- The fixed high speed camera enabled us to capture the region of surge transition, where energy is transferred between the blue and red fluids.
- Stills from two experiments with 90% concentration, but different t_{re} are displayed in Figure 8 & 9, respectively.

Experimental modelling conclusions

- Dilution due to turbulent mixing, erosion and wave instability were all present in the series of experiments. However, they were only efficient for the lowest concentration considered and even then, the dilution was dominant towards the head.
- The surge caused a rapid laminar to turbulent transition at the head for 80% concentration. For lower concentration the head has already diluted before the surge arrived, whereas for higher concentration the surge did not transfer enough energy for a rapid transformation.

Figure 8: Evolution of flow filmed with the high speed camera between 12 and 70 cm downstream. Glycerol concentration 90% and gate separation time 3.3 s. Scale in cm.

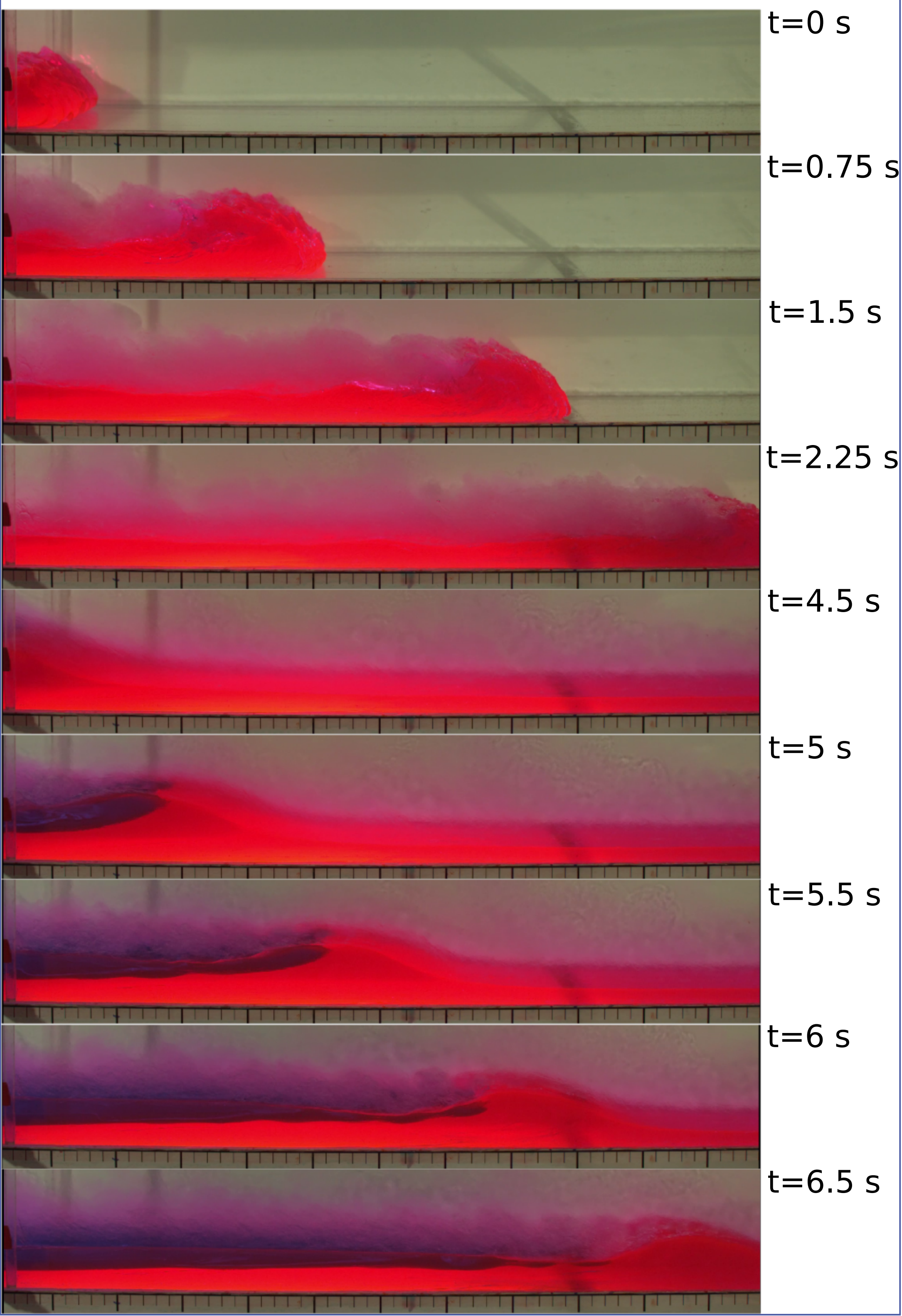
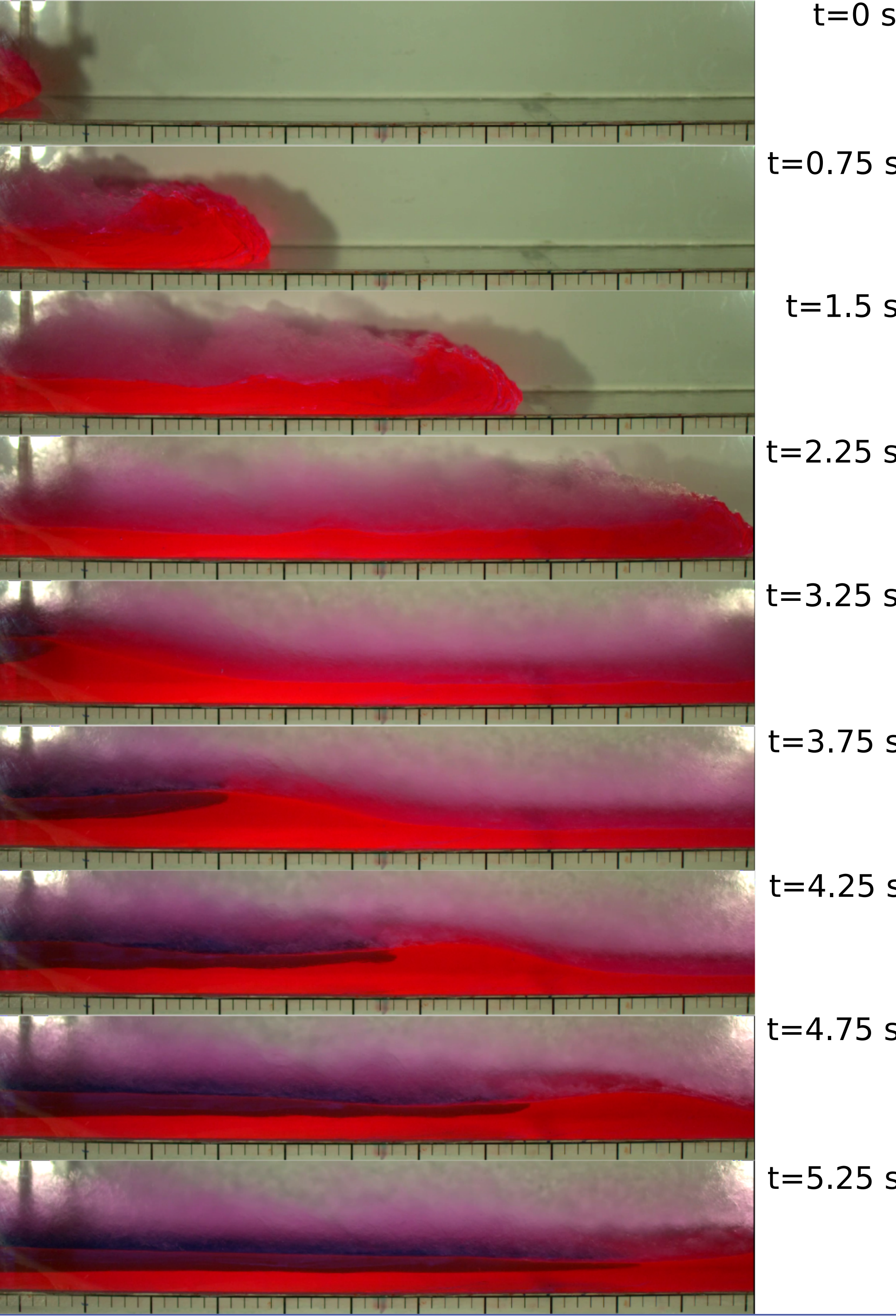


Figure 9: Evolution of flow filmed with the high speed camera between 12 and 70 cm downstream. Glycerol concentration 90% and gate separation time 1.3 s. Scale in cm.



3. Numerical modelling

- The long and thin nature of the flow was exploited to use the depth-averaged shallow-water equations (1), where h is the depth, u is the depth-averaged horizontal velocity, t is time and x is horizontal distance expressed in dimensionless units. The equations were solved using a Lax-Wendroff finite-difference scheme [3].
- Initial (2) and boundary (3) conditions were imposed reflecting the experimental configuration.
- The shallow-water equations are inviscid and neglect all vertical gradients in the flow; an assumption that breaks down at the head. A Froude number condition, was imposed (4) to capture the neglected dissipation at the head.
- This set of equations are hyperbolic and so can be analysed using the method of characteristics. The equations are recast in terms of two combined quantities $\alpha = u + 2\sqrt{h}$ and $\beta = u - 2\sqrt{h}$. These quantities are conserved along particular lines through (x, t) -space (known as characteristics) given in (5). The conserved value is determined from the starting point; either at $t = 0$, internally, or a boundary for $t > 0$.
- The solution domain can be split into three types of regions:
 - U_i - Uniform region: both α and β are constant;
 - S_i - Simple region: one of α or β are varying;
 - C_i - Complex region: both α and β are varying.

$$\frac{\partial h}{\partial t} + \frac{\partial}{\partial x}(hu) = 0 \quad (1)$$

$$\frac{\partial}{\partial t}(hu) + \frac{\partial}{\partial x}\left(hu^2 + \frac{h^2}{2}\right) = 0. \quad (2)$$

$$h(x, 0) = \begin{cases} 1 & \text{if } x \in [0, 2], \\ 0 & \text{if } x > 2. \end{cases} \quad (2)$$

$$u(0, t) = 0 \quad \forall t, \quad (3)$$

$$u(1, t) = 0 \quad \forall t \leq t_{re}. \quad (3)$$

$$u_N = Frh_N. \quad (4)$$

$$\frac{d}{dt}(u + 2\sqrt{h}) = \frac{d\alpha}{dt} = 0 \quad \text{on} \quad \frac{dx}{dt} = u + \sqrt{h}, \quad (5)$$

$$\frac{d}{dt}(u - 2\sqrt{h}) = \frac{d\beta}{dt} = 0 \quad \text{on} \quad \frac{dx}{dt} = u - \sqrt{h}.$$

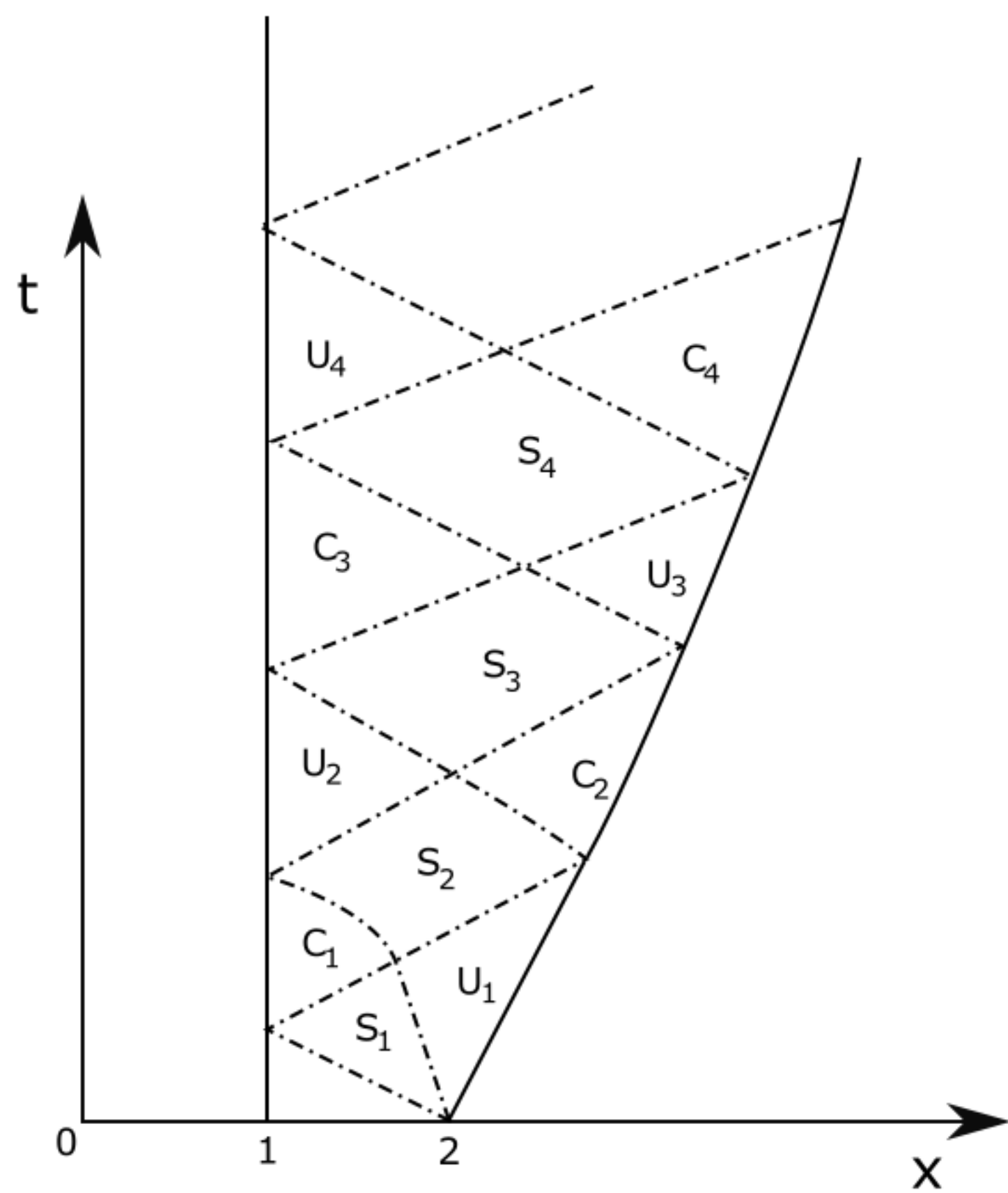


Figure 10: Characteristic diagram before the second gate is release ($t < t_{re}$). For odd i , α is constant in S_i , whereas β is constant for even i .

- In uniform regions both h and u take constant values.
- If initially the surge is (dashed line) released into a uniform region it will move at constant speed, Figure 11. The speed changes upon a dash-dot line, which is a characteristic denoting the change to a simple region.
- The speed changes again when it crosses the other dash-dot line.
- The reflection of the backwards travelling disturbance (dotted line) signifies the furthest point affected by the finite length of the domain.
- The shock may (F) or may not (N) be affected by the finite length of the domain, Figure 11. The depth at sample times is displayed in Figure 12
- The shock rapidly decelerates when it is affected by the finite length of the domain ('o'), Figure 11.

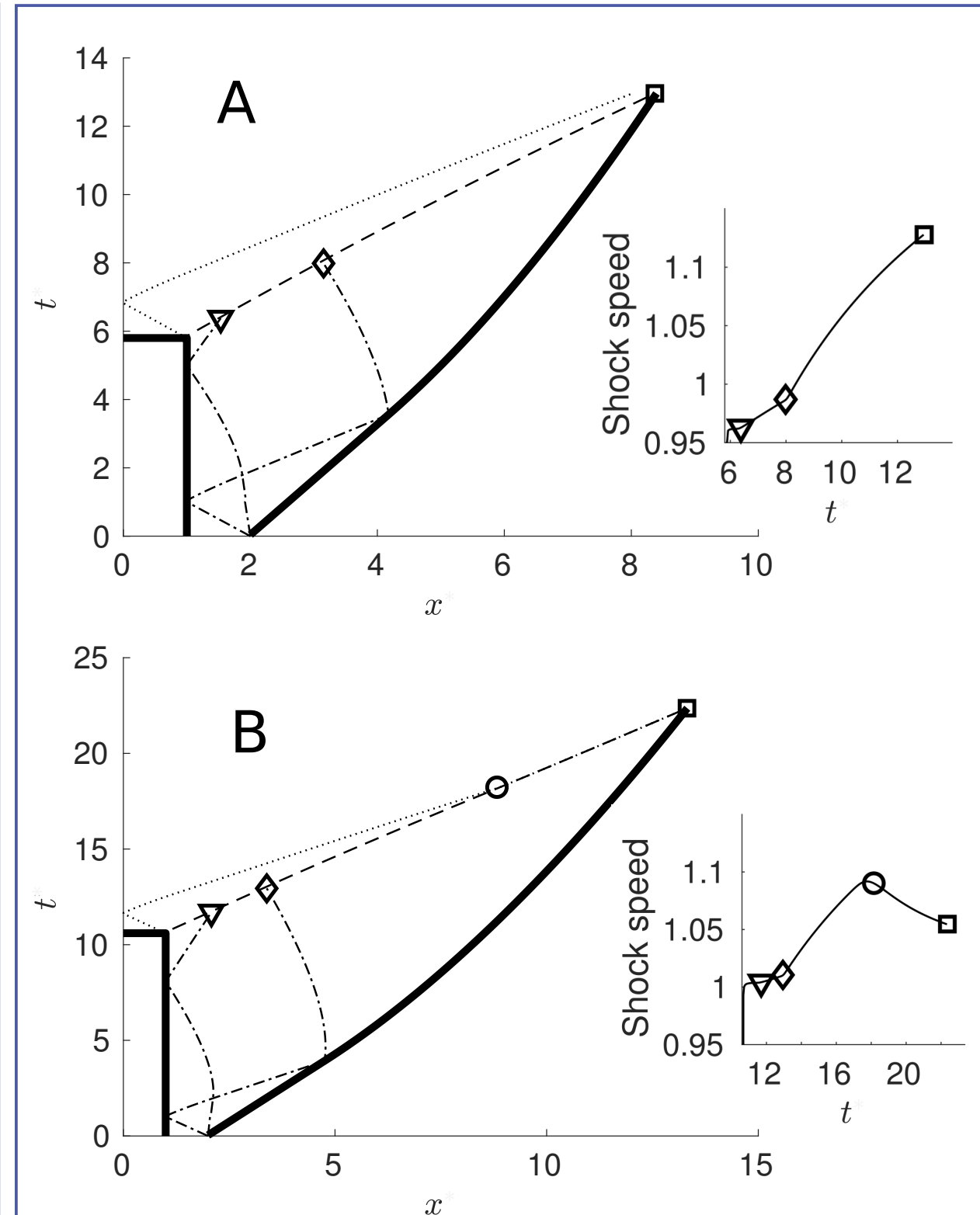


Figure 11: Characteristic diagrams for two cases: Top ($Fr=1.1$ and $t_{re}=10.6$), the shock is affected by the finite length of the domain; Bottom ($Fr=0.9$ and $t_{re}=5.8$), the is unaffected by the finite length of the domain. Inserts display the shock speed (dashed line) for $t > t_{re}$.

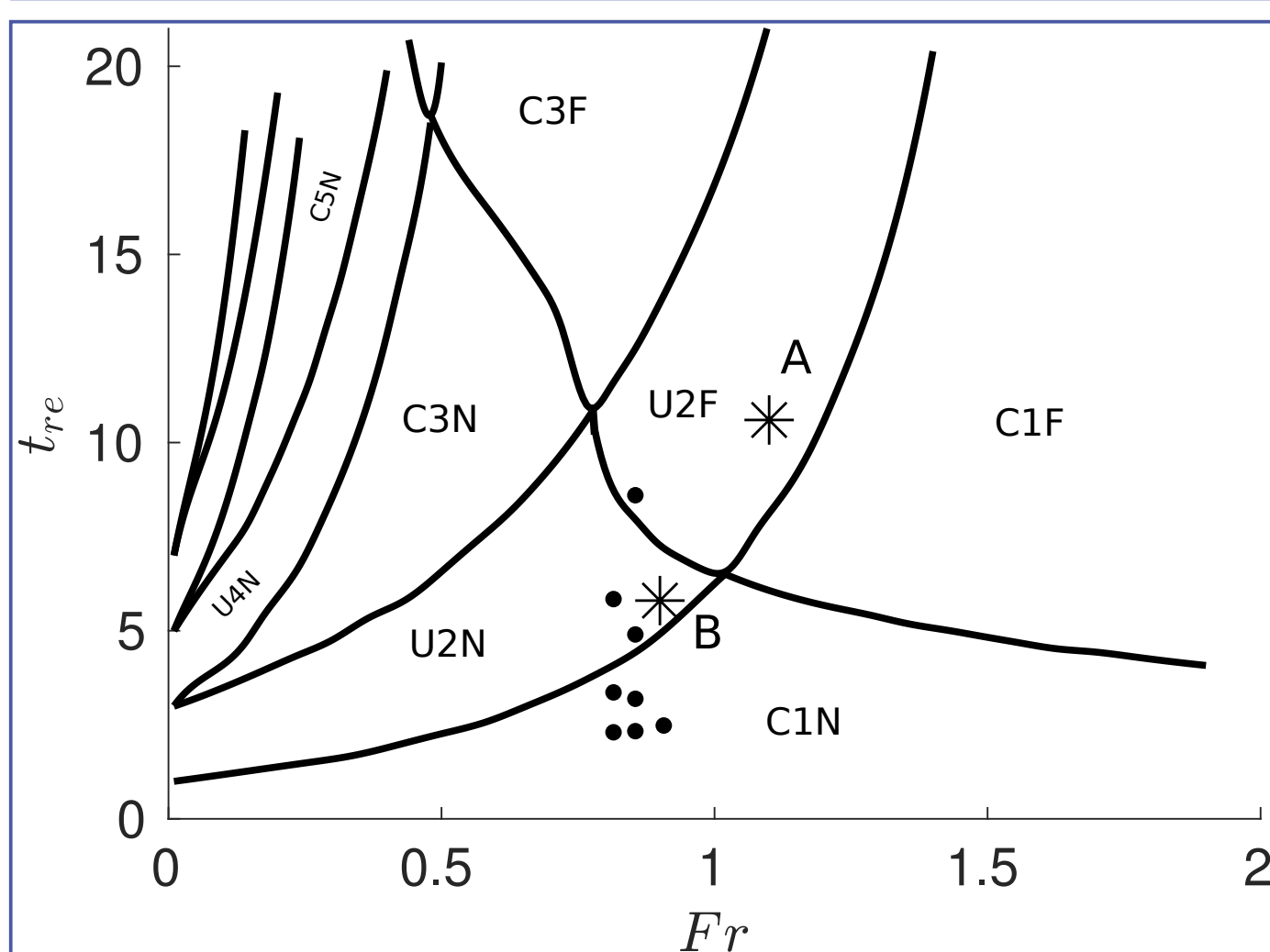


Figure 13: Parameter space demonstrating the first few qualitatively different solutions produced by the numerical model. Asterisks indicate the two cases from Figure 11. Dots represent the experiments. Cases are classified by whether they are affected by the backwards travelling disturbance (F) or not (N) and the region the shock is released into.

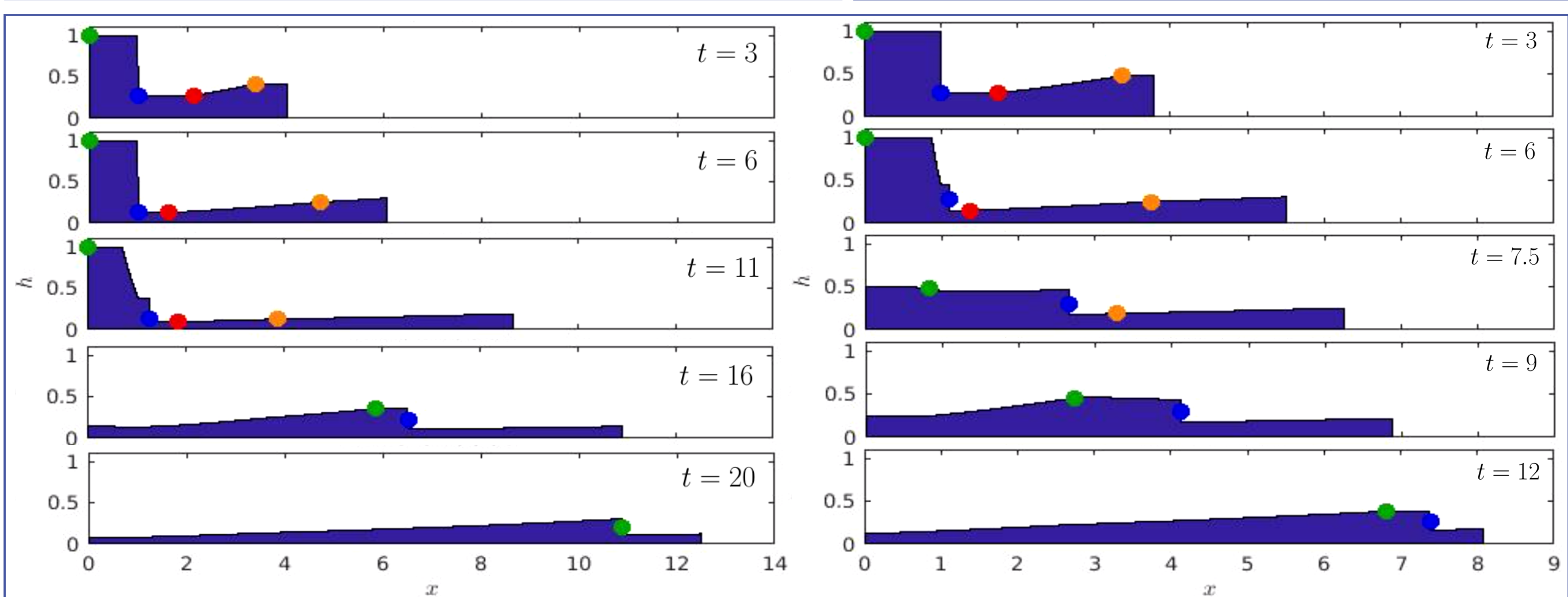


Figure 12: Depth profiles at sample times for the two cases considered: (left) $Fr=1.1$ and $t_{re}=10.6$ and (right) $Fr=0.9$ and $t_{re}=5.8$. The dots indicate the location of key characteristic lines: Red and orange - the boundaries between uniform, simple and complex regions (dash-dot line); Blue - the shock (dashed line); and green the reflection of the backwards travelling disturbance (dotted line).

Numerical modelling conclusions

- The solution is dependent on two parameter, Fr and t_{re} . Qualitatively different solution exist in different regions of the parameter space, Figure 13.
- The shock speed is dependent on the solution structure of the first release and may contain regions of constant speed.
- If the shock is affected by the finite length of the domain its velocity decreases. The speed of the internal shock is critical to internal erosion and deposition of a debris flow.

Future work

- Use the numerical model to interpret the experimental data and relate this to the observed transformation mechanisms.
- Extend the numerical to include sediment transport and non-Newtonian rheology and compare to real world flows.